Dynamic path modification for car-like nonholonomic mobile robots

Conference Paper · May 1997

DOI: 10.1109/ROBOT.1997.606730 · Source: IEEE Xplore

CITATIONS
121

READS
359

4 authors, including:

Majdoleen Khatib
Tel Aviv University
13 PUBLICATIONS **447** CITATIONS
SEE PROFILE

Raja Chatila
Sorbonne Université
203 PUBLICATIONS **5,279** CITATIONS
SEE PROFILE

Jean-Paul Laumond
Laboratoire d'Analyse et d'Architecture des Systèmes (LAAS)
244 PUBLICATIONS **9,662** CITATIONS
SEE PROFILE

Proceedings of the 1997 IEEE
International Conference on Robotics and Automation
Albuquerque, New Mexico - April 1997

Dynamic Path Modification for Car-Like Nonholonomic Mobile Robots

M. Khatib, H. Jaouni, R. Chatila, J.P. Laumond
LAAS-CNRS
7, Avenue du Colonel Roche, 31077 Toulouse Cedex 4 France
e-mail : {maher, hazem, raja, jpl}@laas.fr

Abstract

In this paper, a method combining planning and reactive control for car-like nonholonomic mobile robots is discussed. Firstly, a "bubble" for a car-like mobile robot is defined as the locally reachable space from a given configuration considering the obstacles and using the appropriate metric. Then a flexible feasible trajectory, based on the *elastic band* concepts, is constructed. This trajectory is smoothed using Bezier curves satisfying a minimum curvature constraint, and a parameterization is proposed which satisfies the robot kinematics constraints.

1 Introduction

This paper presents a method for on-line modification of nonholonomic mobile robot trajectories to comply with environmental changes, while guaranteeing its feasibility (respecting robot dynamics) and goal reachability.

This problem was addressed by several authors. Krogh and Thorpe [3] proposed to replace the planned trajectory by critical points. The artificial potential field method [6] is then applied to move the robot between these points. The drawbacks of this method is that the robot does not move on a known trajectory, and hence its motion between the critical points is not known and more difficult to control.

Choi [12] introduced the *channel* concept to represent the trajectory. A channel is defined by a sequence of adjacent configurations in free-space joining the initial and goal configurations. A potential field is defined to guide the robot along the channel to the goal position. However, the off-line construction of channels prevents from taking into account subsequent changes in the environment. In addition, this method is developed for a holonomic robot and no direct way was proposed to adapt it to nonholonomic mobile robots.

Quinlan and Khatib [8] proposed a dynamic trajectory modification concept called the *elastic band*, which consists in maintaining a permanent flexible and deformable path between the initial and goal configurations. The path is paved with "bubbles". A bubble represents the local free-space around a given configuration of the robot up to the closest obstacle. This method is defined for holonomic robots, and does not deal with nonholonomy. Nevertheless, it has the advantage of being entirely based on distance functions.

Taking advantage of this property, we propose a nonholonomic bubble band implemented for car-like robots, using an appropriate metric space. To begin with, we present the original bubble band approach. Then our generalization to a nonholonomic robot is developed in section 3. The path produced by the method being a sequence of lines and arcs of circle, a smoothing method based on Bezier polynomials is presented in section 4 to transform it into a kinematically feasible trajectory. Experimental results are shown and discussed in section 5.

2 The Bubble Band Concept

A bubble, as introduced in [7], represents the maximum local subset of the free-space around a given configuration of the robot which can be traveled in any direction without collision. It is generated from distance information about the robot model and the objects in the environment. Bubbles enable the treatment of free-space information without computing and representing the entire free-space.

Using bubbles we can guarantee collision-free paths. Given $\{\mathbf{p}_i\}_{i=1...n}$ configurations in free-space such that the bubbles defined around two consecutive configurations, $B(\mathbf{p}_i)$ and $B(\mathbf{p}_{i+1})$ overlap, it is possible to construct a collision-free path from $\mathbf{p}_1$ to $\mathbf{p}_n$. This path is an elastic band paved with bubbles, or a bubble band. This band will be deformed according to

two kinds of forces: internal and external.

This means that the motion of each configuration in the path is determined by calculating a force composed of these two parts. The internal forces act to remove slack in the band (energy minimization), the external forces move the band away from obstacles (thus maintaining the path collision free).

To maintain the band in free-space we should insure that adjacent bubbles overlap. Before two adjacent bubbles become disconnected because of the action of the forces, a new bubble is created between them. Another modification is to remove redundant bubbles. If two non-adjacent bubbles overlap, all the intermediate bubbles are suppressed from the band.

3 Nonholonomic Bubble Band

3.1 Nonholonomic bubble

Here, we present the metric space associated with a car-like nonholonomic mobile robot having a non-null minimal steering radius R. A configuration of the robot is defined in the space $\mathcal{R}^2 \times \mathcal{S}^1$. It has been proven that a shortest path between two configurations belongs to one of 48 simple sequences of at most five pieces, each piece being a straight line segment, or an arc of a circle, with at most two cusp points [9]. The length of the shortest paths were equips the configuration space $\mathcal{R}^2 \times \mathcal{S}^1$ with metric structure compatible with the robot movement [4]. This distance is denoted by d.

Definition 3.1 A *bubble* $B(\mathbf{p}, r)$ of *center* $\mathbf{p}$ and *radius* r is the set of configurations at a distance smaller than r from $\mathbf{p}$

$$B(\mathbf{p}, r) = \{\mathbf{q} \in \mathcal{R}^2 \times \mathcal{S}^1 \mid d(\mathbf{p}, \mathbf{q}) < r\}.$$

Definition 3.2 Two bubbles $B(\mathbf{p}, r)$ and $B(\mathbf{q}, s)$ are said to be *connected* if

$$B(\mathbf{p}, r) \cap B(\mathbf{q}, s) \neq \emptyset.$$

It follows that two bubbles $B(\mathbf{p}, r)$ and $B(\mathbf{q}, s)$ are connected if and only if

$$d(\mathbf{p}, \mathbf{q}) < r + s.$$

As a consequence, a Reeds and Shepp path, $\gamma[\mathbf{p}, \mathbf{q}]$, joining the two centers of connected bubbles is wholly included in the union of these bubbles.

This property enables us to prove the existence of a feasible path from the initial configuration to the final configuration by finding a sequence of connected bubbles joining both configurations (fig. 1).

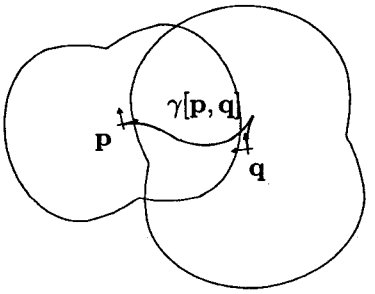

Figure 1: *Path between two consecutive centers*

A bubble may be of two types, *movable* or *immovable*. A movable bubble is a bubble whose center can be modified according to the forces applied to it. An immovable bubble keeps the same center throughout the execution (for example the start configuration or the goal when it is fixed).

A bubble is said to be smaller than another if they have the same center and if the first is wholly included in the second.

Based on [10], the problem of the distance between a robot configuration and a point or segment obstacle was solved [11].

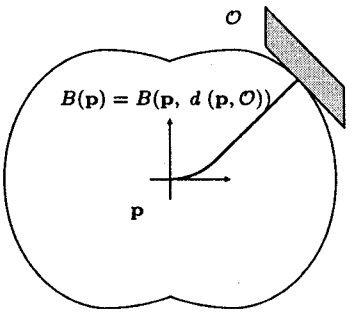

Figure 2: *Biggest collision-free bubble.*

This allows to define the biggest collision-free bubble around a configuration as $B(\mathbf{p}) = B(\mathbf{p}, d(\mathbf{p}, \mathcal{O}))$, where $\mathcal{O}$ is the set of segment obstacles (fig. 2).

Let us now introduce the various forces to be applied to a connected sequence of bubbles, so called *bubble band.*

3.2 Forces

The forces applied to the bubbles are of two essential types. The external forces due to the repulsion of the obstacles and the internal forces which work to keep the bubbles connected, as long as possible, and optimize the form of the band.

3.2.1 Internal Forces

How should the bubbles interact with each other? This is a crucial question because once the inter-bubble interactions determined, they can be translated into potential fields, which in their turn determine the internal forces of the bubble band. In this subsection $B(\mathbf{p_{i-1}}, r_{i-1})$, $B(\mathbf{p}_i, r_i)$ and $B(\mathbf{p}_{i+1}, r_{i+1})$ are three consecutive bubbles in a bubble band.

Firstly, adjacent bubbles should remain connected. That is

$$d^+(\mathbf{p}_i) = d(\mathbf{p}_i, \mathbf{p}_{i+1}) \leq r_i + r_{i+1} - \epsilon_c. \qquad (1)$$

for some small $\epsilon_c \in \mathcal{R}^{+*}$.

Secondly, adjacent bubbles should not overlap too much lest the band tends to be over charged uselessly with bubbles, with consequent effects on the efficiency of the method. Thus

$$d^+(\mathbf{p}_i) = d(\mathbf{p}_i, \mathbf{p}_{i+1}) \geq r_i + r_{i+1} - \epsilon_o, \qquad (2)$$

for some small $\epsilon_o \in \mathcal{R}^{+*}$ greater than ϵ_c.

Finally, the band should tend to contract. Away from obstacles it should even be a straight band. Thus the center of a middle bubble should try to place itself on a shortest path joining its two neighboring centers on the radius-weighed barycenter of these centers. If $\gamma_p[\mathbf{p}_{i-1}, \mathbf{p}_{i+1}] : [0,1] \longrightarrow \mathcal{R}^2 \times \mathcal{S}^1$ is a parameterization of $\gamma[\mathbf{p}_{i-1}, \mathbf{p}_{i+1}]$, the path joining $\mathbf{p}_{i-1}$ and $\mathbf{p}_{i+1}$, and if $\tilde{r}_i = \frac{r_{i-1}}{r_{i-1}+r_{i+1}}$, then

$$d^\gamma(\mathbf{p}_i) = d(\mathbf{p}_i, \gamma_p[\mathbf{p}_{i-1}, \mathbf{p}_{i+1}](\tilde{r}_i)) \leq \epsilon. \qquad (3)$$

where $\epsilon \in \mathcal{R}^+$ is arbitrarily small.

Using the constraints 1 to 3 and noting $d^-(\mathbf{p}_i) = d^+(\mathbf{p}_{i-1})$, the following potential fields are deduced

$$\begin{aligned}
\mathcal{P}_f(\mathbf{p}_i) &= \frac{K_f}{2}\Big(d^+(\mathbf{p}_i) - (r_i + r_{i+1}) + \epsilon_c\Big) \\
&\quad \times \Big(d^+(\mathbf{p}_i) - (r_i + r_{i+1}) + \epsilon_o\Big) \\
\mathcal{P}_b(\mathbf{p}_i) &= \frac{K_b}{2}\Big(d^-(\mathbf{p}_i) - (r_{i-1} + r_i) + \epsilon_c\Big) \\
&\quad \times \Big(d^-(\mathbf{p}_i) - (r_{i-1} + r_i) + \epsilon_o\Big) \qquad (4) \\
\mathcal{P}_c(\mathbf{p}_i) &= \frac{K_c}{2}\Big(d^\gamma(\mathbf{p}_i)\Big)^2.
\end{aligned}$$

where $\mathcal{P}_f$ is the forward connection potential, with the next bubble, $\mathcal{P}_b$ is the backward connection potential and $\mathcal{P}_c$ is the contraction potential.

3.2.2 External Forces

The bubble band should alway evolve in free-space. In presence of mobile or immobile obstacles some interaction should take place to guarantee a collision-free band. These interactions are performed by external repulsive forces, function of the distance to obstacles. These forces can be simply derived from repulsive potential fields such as developed in [2].

The application of the $-\nabla$ operator to derive the force expressions from the previously defined potentials, brings us to calculate $\frac{\partial d}{\partial \mathbf{p}}$ where $\mathbf{p}$ is the configuration that varies. In fact this last expression gives the direction of the force. Unlike the Euclidean distance, the car-like compatible distances, defined previously, have no normalized differentials. They contribute thus to the magnitude of the force. As well, they do not vary smoothly with $\mathbf{p}$, with consequent effects on stability (see section 3.4).

3.3 Creation and Modification of a Bubble Band

As the band expands, bubbles should be created to guarantee the connectivity. Bubbles are also created when an obstacle approaches the band obliging the bubbles to shrink. Inversely, when the band is contracted or when obstacles move away, bubbles may overlap too much, so that some of them should be eliminated.

3.3.1 Bubble Band Creation

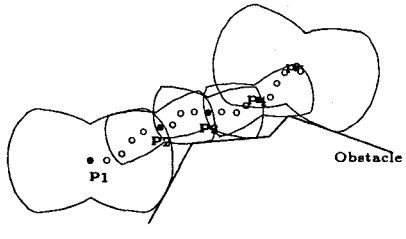

Figure 3: *Creation of the first bubble band.*

To construct the original band (fig. 3), we start with a path, which may be given by a motion planner. This path is firstly sampled into a sequence of configurations. Then the first bubble is defined to be the greatest bubble centered at the first configuration in the sequence. The sequence is then scanned, by dichotomy, to find the last configuration which still belongs to the last constructed bubble. This configuration is thus taken to be the center of the following bubble which also has the maximum size. The previous step is repeated till the goal (the last configuration) is found to belong to a bubble. This method insures the connectivity of the bubble band, as well as its total presence in free-space while making it redundant, obliging the center of each bubble, but the

first, to belong to its previous neighbor. Nevertheless, this redundancy is not an inconvenience, for after the first application of the elimination algorithm and of the contraction forces, the band will become spacious.

3.3.2 Bubble Band Modification

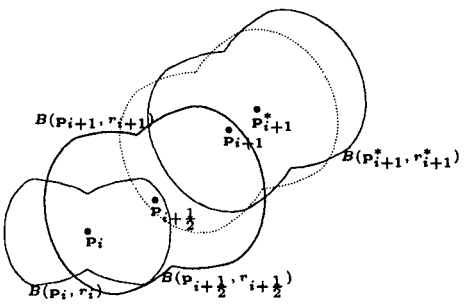

Figure 4: *Creation of a bubble before disconnection.*

Suppose we have a connex bubble band. For each two adjacent bubbles, say $B(\mathbf{p}_i, r_i)$ and $B(\mathbf{p}_{i+1}, r_{i+1})$, if the following inequality is satisfied

$$d(\mathbf{p}_i, \mathbf{p}_{i+1}) \geq r_i + r_{i+1} - \epsilon_c,$$

where ϵ_c is a positive constant, then an intermediate bubble should be created between them (fig 4). In order to be around the intersection of its two neighbors, the center of this bubble should be on the path, $\gamma_p[\mathbf{p}_i, \mathbf{p}_{i+1}] : [0,1] \longrightarrow \mathcal{R}^2 \times \mathcal{S}^1$, relating the two neighboring centers; on the point

$$\mathbf{p}_{i+\frac{1}{2}} = \gamma_p[\mathbf{p}_i, \mathbf{p}_{i+1}] \left(\frac{r_i}{r_i + r_{i+1}} \right).$$

On the other hand, if three consecutive bubbles, $B(\mathbf{p}_{i-1}, r_{i-1})$, $B(\mathbf{p}_i, r_i)$ and $B(\mathbf{p}_{i+1}, r_{i+1})$ have the property

$$d(\mathbf{p}_{i-1}, \mathbf{p}_{i+1}) \leq r_{i-1} + r_{i+1} - \epsilon_o,$$

where $\epsilon_o > 0$, then they are considered to be redundant and the middle bubble $B(\mathbf{p}_i, r_i)$ is eliminated.

To prevent the creation-elimination loop from endlessly creating and eliminating the same bubble, the following condition should be satisfied

$$\epsilon_o > \epsilon_c. \tag{5}$$

3.4 Stability

The evolution of the bubbles in the band is governed by conservative forces issued from convex potential fields. For contraction forces, the potential fields are functions of the metric distance which is a true distance and conserves thus the convexity property. These potential fields have thus a unique minimum.

For obstacle repulsion forces, the potential fields are functions of the configuration to point distance which is not a true distance. In fact, this distance presents a problem for lengths inferior to $\sqrt{2}R$, as discussed in sub-section 3.2.2. This is due to the discontinuity of the differential of this distance and to the fact that the shortest path, from a configuration to *a point*, does not have the property: *All subpaths of shortest paths are shortest paths.* In fact, subpaths of length inferior to $\sqrt{2}R$ may not be shortest paths.

To guarantee the convergence of the bubble band we impose thus a minimum radius, $R_{\min} = \sqrt{2}R$, on the bubbles.

As for the creation-elimination method, a hysteresis function (equ. 5) around the minimum of the contraction force is used to prevent endless creation-elimination loops.

4 Smoothing and Execution

From now on, we work with the car-like nonholonomic mobile robot metric space.

Once the bubble band is set, the path to execute is the concatenation of the Reeds and Shepp paths $\{\gamma[\mathbf{p}_i, \mathbf{p}_{i+1}], i = 1 \ldots n-1\}$ between the centers of the n bubbles. Each of these paths is a set of arcs and segments and its curvature is thus discontinuous forcing the robot to stop at the end of each piece. Several method are being used currently to smooth these paths. Here we use Bezier polynomials. The advantage of Bezier polynomials is that they can be wholly defined in a convex envelop as well as their derivatives. We can thus guarantee that the path executed lies in the union of the bubbles, and thus in free-space. As well the velocity and acceleration on these curves are bounded, for each belongs to a convex envelop of a finite number of constant vectors.

The only measure that cannot be bounded is the curvature. Here we choose a set of control points to insure that the curvature lies in the neighborhood of R, the steering radius.

4.1 Approximation by Bezier Curves

Definition 4.1 A Bezier curve of *order* $n+1$ and *control points* $\mathbf{p} = \{\mathbf{p}_0, \ldots, \mathbf{p}_n\}$ is defined by

$$\mathcal{BP}[\mathbf{p}](t) = \sum_{i=0}^{n} B_i^n(t)\mathbf{p}_i,$$

where $B_i^n(t) = \binom{n}{i} (1-t)^{n-i} t^i, \qquad \text{for } i = 0 \ldots n.$

We use the following properties of Bezier curves (for a full development see [1].)

- A Bezier curve lies in the convex envelop of its control points $\mathcal{BP}[\mathbf{p}] \subset \text{co}(\mathbf{p})$.
- The derivative of a Bezier curve is a Bezier curve whose control points are finite differences of the original control points.

According to the first property, choosing the control points in a bubble or, a region, guarantees that all the curve is in that bubble, or region.

The second property combined with the first one insures that the derivatives $\frac{\partial^k}{\partial t^k}\mathcal{BP}[\mathbf{p}]$ are contained in the convex envelops $\text{co}(\Delta^k\mathbf{p})$ and thus that the velocity and the acceleration are bounded.

Reeds and Shepp paths are made up of line segments and arcs of circles. To join them smoothly, we will approximate the arcs by Bezier curves whose curvature is null at the two extremities. To satisfy this condition and fix the starting and finish positions and velocities we need at least six control points ($\mathbf{p}_i$, for $i = 0 \ldots 5$) set in the following way. At each extremity; the first point is on the extremity, the second in the direction of the velocity and the third collinear to preceding two, to insure null curvature. Since the initial and end velocities can be controlled by an appropriate parameterization, we are left with four distances to determine. Due to symmetry, these four degrees of freedom are reduced to two: $l = |\overline{\mathbf{p_0}\,\mathbf{p_1}}| = |\overline{\mathbf{p_4}\,\mathbf{p_5}}|$ and $k = |\overline{\mathbf{p_1}\,\mathbf{p_2}}| = |\overline{\mathbf{p_3}\,\mathbf{p_4}}|$.

The problem is thus reduced to

$$\min_{l>0,k>0} \max_{t\in[0,1]} \frac{\|\mathcal{BP}'[\mathbf{p}](t) \times \mathcal{BP}''[\mathbf{p}](t)\|}{\|\mathcal{BP}'[\mathbf{p}](t)\|^3}.$$

This optimization problem has not been solved yet. For the time being; we use values of l and k that bound the curvature to $\frac{6}{5}\rho$ where ρ is the curvature of the arc ($\rho = \frac{1}{R}$ if R is the steering radius).

4.2 Parameterization of Bezier Curves

The parameters l and k determine the shape of a Bezier curve. This curve can then be followed in different ways by changing its parameterization. In fact, if $\varphi : [t_0, t_1] \longrightarrow [0, 1]$ is a strictly increasing onto function, except perhaps on t_0 and/or t_1 then $t \longrightarrow \mathcal{BP}[\mathbf{p}](\varphi(t))$, is a new parameterization of $\mathcal{BP}[\mathbf{p}]$. If we have a predetermined starting velocity v_s, this parameterization should verify

$$\mathcal{BP}'[\mathbf{p}](\varphi(t_0))\frac{\partial}{\partial t}\varphi(t_0) = v_s.$$

Similarly, if the finishing velocity is known,

$$\mathcal{BP}'[\mathbf{p}](\varphi(t_1))\frac{\partial}{\partial t}\varphi(t_1) = v_{finish}.$$

The reparameterization can also be used to modify the maximum velocity. In fact, due to the convex envelop property, to guarantee that the velocity does not exceed v_{max}, φ should verify

$$\left|\frac{\partial}{\partial t}\varphi(t)\right| \leq \frac{v_{max}}{5 \max\limits_{i=0\ldots4} \|\Delta\mathbf{q}_i\|}, \qquad \forall t \in [t_0, t_1].$$

A similar reasoning can also be applied to bound the acceleration, the angular velocity and the angular acceleration (details in [5]).

5 Implementation and Experimental Results

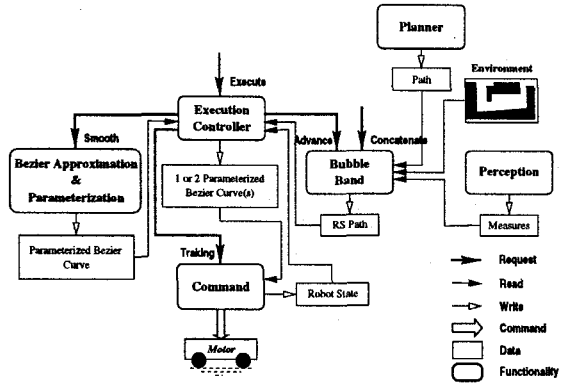

Figure 5: *Architecture of the* Kinan *system*

The algorithms and approach described above are implemented in an architecture called Kinan[1] (fig. 5). A planner, using an environment model, generates a trajectory connecting the initial and goal positions, which is not necessary feasible. It is passed to the bubble band module.

First of all, the bubble band sampling algorithm generates a sequence of bubbles connecting the two extremities, replacing thus the original trajectory (fig. 6). The band is then exposed to forces (fig. 7). While executing the band piecewise, it reacts to the modification of the environment (fig. 8). Note that the algorithm work on the analytical representations. The environment and the trajectory are not represented in a bitmap structure. There is hence no limitations on the size of the workspace.

6 Conclusion

Combining planning and reactive control for car-like nonholonomic mobile robots is hereby discussed.

[1] Kinan: Kinematics Integrated in nonholonomic Autonomous Navigation.

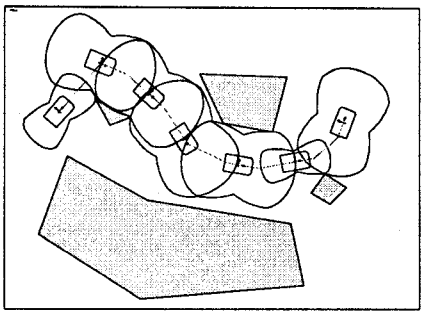

Figure 6: *First bubble band creation.*

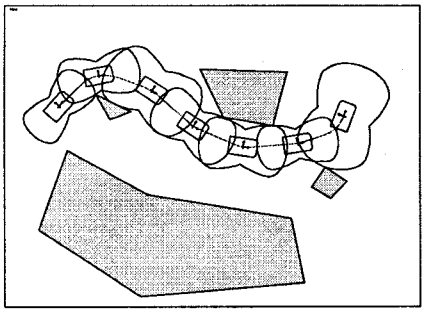

Figure 7: *Bubble band under total forces.*

A bubble for a point car-like mobile robot is defined using the appropriate metric. A flexible feasible trajectory, based on the *elastic band* concepts, is constructed. This trajectory is smoothed using a Bezier technique satisfying the curvature constraint. A parameterization is proposed which satisfies the robot kinematic constraints. A simulation system is developed to evaluate the capabilities of this approach.

This approach was fully developed for a point car-like mobile robots. To take into account the robot form, we have increased the minimum size of bubbles to include the robot. This size represents the maximum distance between the robot center and its boundaries. This is not satisfactory, overconstraining the freedom of bubbles, specially that the method can be generalized just by defining a distance function taking into account the real form of the robot.

Acknowledgment Thanks to M. Vendittelli for her help on one of the distance computation algorithms.

References

[1] J. Fiorot and P. Jeannin. *Courbes et surfaces rationelles.* Masson, Paris, 1989.

[2] M. Khatib. *Sensor-based motion control for mobile robots.* PhD thesis, LAAS-CNRS, Toulouse, France, December 1996. – Ref.: 96510.

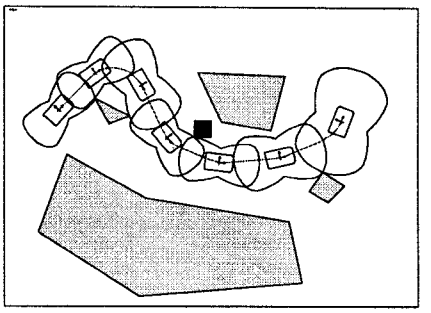

Figure 8: *Bubble band deformation to avoid a mobile obstacle.*

[3] B.H. Krogh and C.E. Thorpe. Integrated path planning and dynamic steering control for autonomous vehicles. In *Proc. IEEE International Conference on Robotics and Automation, San Francisco (USA).*, 1986.

[4] J.-P. Laumond and P. Souères. Metric induced by the shortest paths for a car-like mobile robot. In *IEEE International Workshop On Intelligent Robots and Systems, Yokohoma, (Japan)*, 1993.

[5] M. Khatib and H. Jaouni. Kinematics integrated in non-holonomic autonomous navigation. Technical Report 96346, LAAS-CNRS, September 1996.

[6] O. Khatib. Real-time obstacle avoidance for manipulators and mobile robots. *The International Journal of Robotics Research*, 5(1):90–98, 1986.

[7] S. Quinlan. *Real-Time Collision-Free Path Modification.* PhD thesis, Stanford University, CS Departement, January 1995.

[8] S. Quinlan and O. Khatib. Elastic bands: connecting path planning and control. In *IEEE International Conference on Robotics and Automation, Atlanta, (USA)*, 1993.

[9] J.A. Reeds and L.A. Shepp. Optimal paths for a car that goes both forwards and backwards. *Pacific Journal Mathematics*, 145(2):367–393, 1990.

[10] P. Souères, J.-Y. Fourquet, and J.-P. Laumond. Set of reachable positions for a car. *IEEE Transactions on Automatic Control*, 39(8), August 1994.

[11] M. Vendittelli and J.-P. Laumond. Visible position for car-like robot amidst obstacles. In *Workshop on Algorithmic Foundations of Robotics, WAFR'96*, July 1996.

[12] W. Choi D. J. Zhu and J. C. Latombe. Contingency-tolerant motion planning and control. In *Proceedings of IROS 89*, Tsukuba, Japan, 1989.